

# An Ultra-Wideband THz Absorber Based on Graphene Disks for TM and TE Modes

Omid Mohsen Daraei<sup>1</sup>, Mir Mahdi Safari<sup>2</sup>, and Mohammad Bemani<sup>3,\*</sup>

<sup>1,2,3</sup>*Faculty of Electrical and Computer Engineering, University of Tabriz, Tabriz, Iran*

*\*Corresponding author: bemani@tabrizu.ac.ir*

## Abstract

In this research paper, an unsophisticated configuration of the ultra-wideband THz absorber for transverse electric (TE) and transverse magnetic (TM) modes of the incident THz wave is proposed. The mentioned absorber consists of two layers of graphene disks and one kind of dielectric that is utilized for substrates. Graphene disks with periodic structure have been recently equalized to the analytical circuit model. So, this circuit model is considered for developing the equivalent transmission line model for the whole of the absorber structure. Therefore, the input impedance of the designed absorber is obtained by the equivalent transmission line theory. And also, the real part of the input impedance is approximately regulated to be matched to the free space impedance while the imaginary part of it is closely adjusted to zero around the central frequency of the THz absorber. Using only just two layers of periodic arrays of graphene disks (PAGDs) with one kind of dielectric as the material of substrates, it causes the bandwidth of 90% absorption reached up to 128 % of the central frequency in a THz regime.

**Keywords**— Terahertz; Absorber; Ultra-wideband; Input impedance; Graphene; Transmission line model

## 1. Introduction

With the expansion of THz frequency band, the design of absorbers for the THz region has become an interesting field, which they are used in biosensing, imaging, and communications [1, 2]. Hence, graphene is frequently used in optical fields, based on its special structure and features, such as surface plasmon polariton-based absorption. For describing the structure of this special metamaterial, graphene has a hexagonal lattice configuration, which is made of carbon atoms. Manageable plasmonic features [2, 3], very small thickness and low losses [4], and high-speed operation are some of the characteristics of graphene. Also, another important feature of the graphene-based absorber in comparison with other absorbers is its tunable electrical conductivity by Fermi levels (chemical potentials) [5, 6] that can operate in different ranges of THz frequencies.

In the last years, the design of THz absorbers based on graphene with various shapes have been reported such as square patch [7], stacks [6, 8], and cross-shaped arrays [9]. In the recent research paper [10], a layer of periodic arrays of graphene disks (PAGDs) has been equalized by a series RLC branch. In papers [11] and [12], the narrowband and broadband THz absorbers by utilizing analytical circuit theory have been designed. In this work, the analytical circuit model of PAGDs [10] has been utilized to consider each layer of graphene disks with the period structure as circuit components.

In the recent THz absorbers [13-18], the best-normalized bandwidth of the 90% absorption has been achieved 100% in [18]. In the paper [18], the ultra-broadband THz absorber has been designed in three layers based on periodic arrays of graphene ribbons (PAGRs). In that paper, the number of layers of graphene ribbons has been increased, so it has caused the structure of that THz absorber is more complex. Moreover, in that THz absorber [18], the normalized bandwidth of 90% absorption has been achieved 100% only just for TM mode of the normal incident THz wave, and that has worked over 90% absorption only just for TM mode.

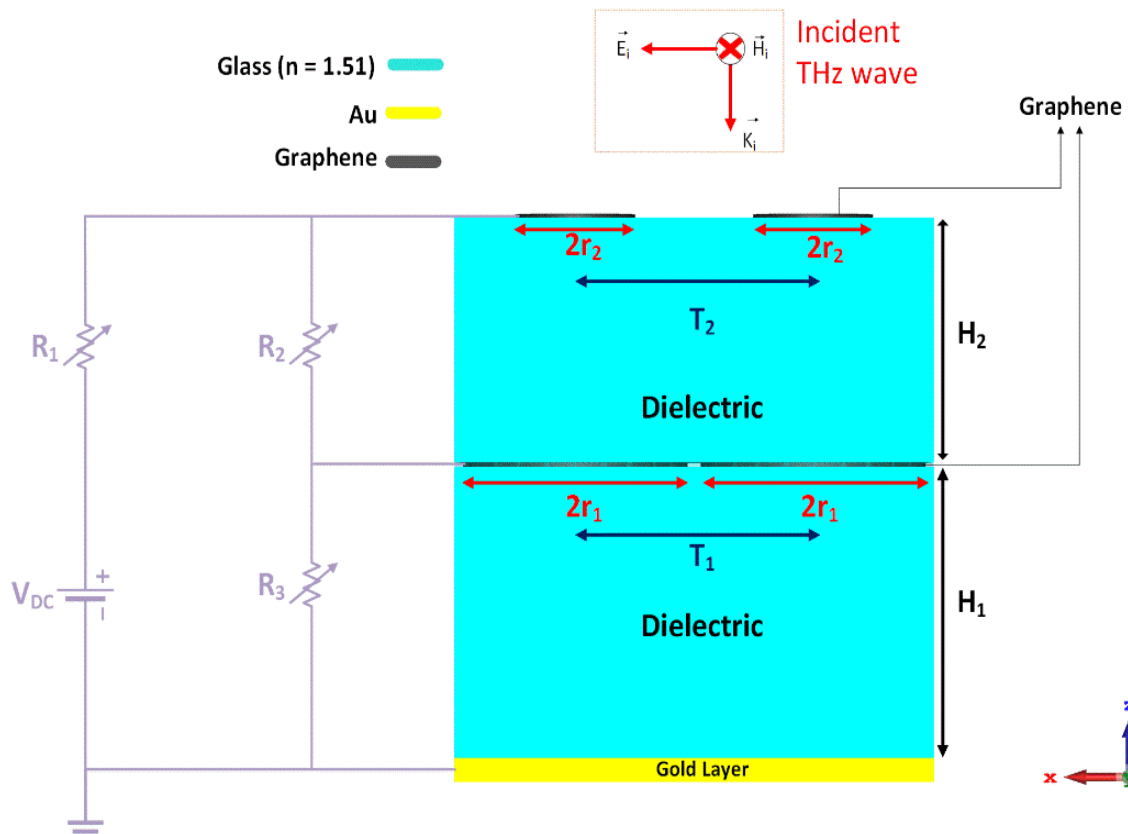
In this work, we have designed an ultra-wideband THz absorber with two layers of PAGDs that has an excellent operation in comparison with previous related works[13-18]. For the design of this THz absorber, the transmission line theory [19, 20] is developed for the whole of the configuration of the proposed absorber that is including two PAGDs as circuit components.

As a result, the bandwidth of 90% absorption is approximately reached up to 1.83 THz for the both TM and TE modes of the normal incident THz wave with 1.43 THz of the central frequency. In conclusion, the normalized bandwidth of 90% absorption is achieved 128% for this proposed ultra-wideband THz absorber. The absorption coefficient and bandwidth of this absorber can be adjusted over a wide range in a THz regime by Fermi levels (chemical potentials). The proposed device was simulated by microwave CST studio, and the transmission line theory and circuit model were calculated by MATLAB codes. The rest of this paper consists of three sections. Section two describes the unit cell structure of the proposed THz absorber and relative circuit model and transmission line theory. In section three, simulation results are analyzed, and the final section concludes the paper.

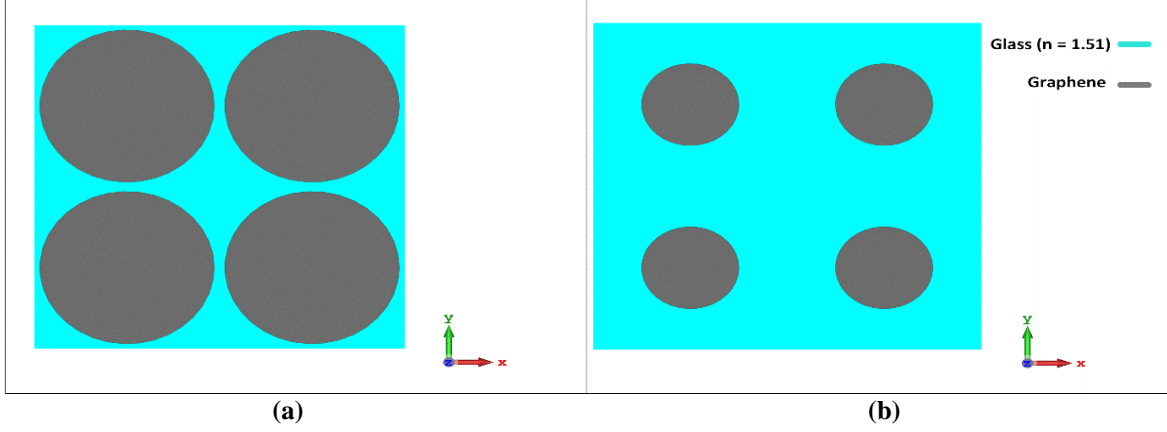
## **2. Structure of Proposed THz Absorber and Relative Circuit Model**

Fig. 1 and Fig. 2 show the side and top views of the unit cell structure of the proposed THz absorber. This absorber is designed of two layers of PAGDs and two substrates with one kind of material. A golden sheet with 1  $\mu\text{m}$  thickness that is used in the bottom of the configuration, it has the metallic ground role, so the incident THz wave cannot transmit through this layer. In other words, the golden sheet acts as a short circuit that can reflect the incident THz wave thoroughly. The first layer of graphene disks and golden sheet are separated by a dielectric material, which has the refractive index  $n_{s1}=1.51$ . And also, the second substrate is composed of the same dielectric material, so it has the same refractive index with the first substrate, which

is located between two PAGDs. Graphene disks on the first substrate have the same radiuses with  $r_1 = 15.1 \mu\text{m}$ , and graphene disks on the second substrate have the same radiuses too with  $r_2 = 8.04 \mu\text{m}$ . The periods of the first and second layers of graphene disks are shown by  $T_1$  and  $T_2$  respectively, and the diameters of disks on the first and second substrates are illustrated by  $2r_1$  and  $2r_2$  respectively. The thickness of graphene disks is assumed with  $t_g = 1 \text{ nm}$ , which is 10 times greater than the thickness of one graphene layer. Calculation of the first substrate thickness can be done by  $H_1 = \frac{c_0}{4n_1f_0}$ , where  $c$  is the speed of light in the free space,  $n_1$  and  $n_2$  are referred to the same refractive indexes for the first and second substrate materials correspondingly, and  $f_0$  is the central THz frequency of the absorber.



**Fig. 1.** The side view of the unit cell configuration of the designed absorber consists of one kind of material for the first and second substrates and two layers of PAGDs.



**Fig. 2. Top views of the unit cell structure of the proposed absorber for (a) the first layer of PAGDs and (b) the second layer of PAGDs.**

The surface electrical conductivity of graphene can be mentioned with two portions by intra-band and inter-band ( $\sigma_{GR} = \sigma_{intra} + \sigma_{inter}$ ), and it can be calculated by Eq. (1). Because of the consideration ( $\hbar\omega/\pi \ll E_F$ ) for THz frequencies, the main part in the surface electrical conductivity is the intra-band section, so the inter-band portion can be neglected in Kubo formula [19, 21, 22]. It should be noticed here that  $E_F$ ,  $\omega$ , and  $h$  are Fermi level (chemical potential), the angular frequency, and Planck constant respectively. Therefore, Kubo formula without inter-band section can be given by Eq. (2).

$$\sigma_{GR} = \frac{e^2 K_B T_K}{\pi \hbar^2 (\tau_{GR}^{-1} + j\omega_{GR})} 2 \text{Ln}[2 \cosh(E_F / 2K_B T_K)] + \frac{e^2}{j4\pi\hbar} \text{Ln}\left[\frac{2E_F - \hbar(\omega - j\tau_{GR}^{-1})}{2E_F + \hbar(\omega - j\tau_{GR}^{-1})}\right] \quad (1)$$

$$\sigma_{GR} = \frac{e^2 K_B T_K}{\pi \hbar^2 (\tau_{GR}^{-1} + j\omega_{GR})} 2 \text{Ln}[2 \cosh(E_F / 2K_B T_K)] \quad (2)$$

Where  $K_B$ ,  $e$ ,  $T_K$ , and  $\tau_{GR}$  refer to the Boltzmann constant, the electron charge, the temperature of the surrounding, and the relaxation time of graphene electron respectively. In this paper, the value of  $T_K$  is supposed with 300 K (room temperature), and  $\tau_{GR}$  is supposed with 0.1 ps.

In the circuit model of PAGDs [10], a serious equivalent RLC branch has been proposed for each layer of graphene disks with periodic configuration, and it can be depicted by Fig. 3(a).

Moreover, the impedances of modeled series RLC branches for the first and second layers of PAGDs are illustrated by  $Z_{GR1}$  and  $Z_{GR2}$  respectively in Fig. 3(a).

For the design of an ultra-broadband THz absorber based on PAGDs, the transmission line theory is developed for the whole structure of the absorber. In Fig. 3(b), the golden sheet is considered by a short circuit, so its impedance is assumed by  $Z_{Au} \approx 0$ , and also the first and second dielectric substrates impedances are achieved by  $Z_{su1} = \frac{Z_0}{n_1}$  and  $Z_{su2} = \frac{Z_0}{n_2}$  correspondingly in the transmission line theory.

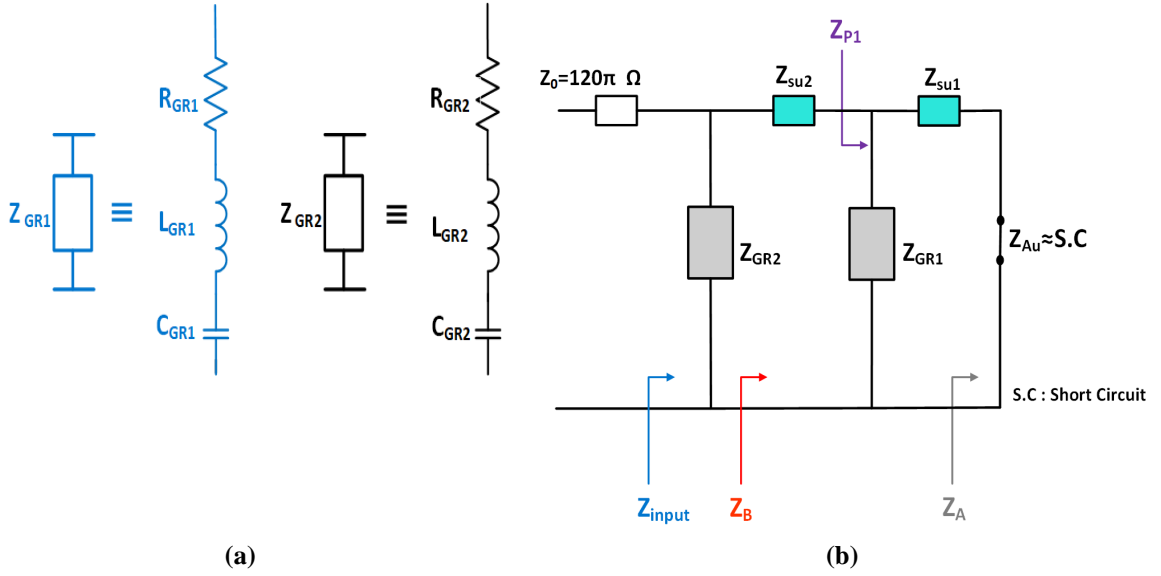


**Fig. 3. (a) The circuit model of the PAGDs and (b) the transmission line model of the mentioned THz absorber.**

For the normal THz incident wave, equivalent impedances for the transmission line model of the proposed absorber can be calculated as:

$$Z_A = jZ_{su1} \tan(\beta_1 H_1) \quad (3)$$

$$Z_{P1} = \frac{Z_{GR1} \cdot Z_A}{Z_{GR1} + Z_A} \quad (4)$$

$$Z_B = Z_{su2} \frac{Z_{P1} + jZ_{su2} \cdot \tan(\beta_2 H_2)}{Z_{su2} + jZ_{P1} \cdot \tan(\beta_2 H_2)} \quad (5)$$

$$Z_{input} = \frac{Z_{GR2} \cdot Z_B}{Z_{GR2} + Z_B} \quad (6)$$

where  $H_1$ ,  $H_2$ ,  $\beta_1$ , and  $\beta_2$  are referred to the thicknesses of the first and second substrates and the propagation constants of the incident THz wave in the first and second substrates respectively. There is a direct relationship between the input impedance of the mentioned absorber and the thicknesses of the substrates. So, for achieving the ultra-wideband absorption, the real part of the input impedance should be approximately adjusted to the free space impedance, and the imaginary part of it should be tuned near zero.

The values of the equivalent resistance, capacitance, inductance, and relaxation time for each layer of the PAGDs have been calculated [10], when they are utilized in the  $n^{\text{th}}$  mode as follows:

$$R_{GR_n} = \frac{K_n T^2 \left(\frac{h}{2\pi}\right)^2}{S_n^2 e^2 \pi E_F \tau_{GR_n}} \quad (7)$$

$$L_{GR_n} = \frac{K_n T^2 \left(\frac{h}{2\pi}\right)^2}{S_n^2 e^2 \pi E_F} \quad (8)$$

$$\tau_{GR_n} = \frac{L_{GR_n}}{R_{GR_n}} \quad (9)$$

$$C_{GR_n} = \frac{\varepsilon_0 \pi^2 S_n^2 (n_{s1}^2 + n_{s2}^2)}{T^2 K_n q_{11}} \quad (10)$$

The values of  $e$  (electron charge) and  $h$  (Planck constant) are equal to  $e \cong 1.602176 \times 10^{-19} [C]$ ,  $h = 6.626 \times 10^{-34} [J.s]$ . In Eq. (10),  $n_{s1}$  and  $n_{s2}$  are the refractive indexes of materials, which they are surrounding the graphene disks, and  $S_n$  could be derived from the integral of the Eigenfunctions in [10]. And also, in Eq. (10),  $q_{11}$  shows the first Eigenvalue of

the equation that can control the surface current density on the graphene disks. Hence, the values of  $q_{11}$  for various  $2r/T$  are illustrated in table 1 of [10]. By considering the only just first mode of the resonance frequency of PAGDs in this paper, the first mode should be focused on the values of  $S_1=0.6087r$  and  $K_1=1.2937$ .

**Table. 1. The calculated Eigenvalues of the equation for controlling the first mode of surface current density on graphene disks [10].**

$2r/T$	0.1	0.5	0.9
$q_{11}r$	0.539	0.527	0.417

Therefore, the resonance angular frequencies of the first and second layers of PAGDs can be evaluated by  $\omega_{0_{GR1}}$  and  $\omega_{0_{GR2}}$  respectively, and they can be written as:

$$\omega_{0_{GR1}} = \frac{1}{\sqrt{L_{GR1} C_{GR1}}} \quad (11)$$

$$\omega_{0_{GR2}} = \frac{1}{\sqrt{L_{GR2} C_{GR2}}} \quad (12)$$

### 3. Simulation Results

In this section, let us evaluate the proposed method for designing a THz absorber through a numerical and simulation procedure. The operation of the ultra-broadband THz absorber based on two layers of PAGDs has been equalized by developing the transmission line model. In this model, the real part of the input impedance has been tuned to be closely matched to  $Z_0$  (the free space impedance) that is equal to  $376.8 \Omega$ , and also the imaginary part of it could be adjusted to near zero around the central frequency of the absorber. The calculated parameters for designing the proposed device have been achieved, and they are demonstrated in table 2.

**Table. 2.** The obtained values of parameters for the design of the proposed THz absorber.

	<i>The 1<sup>st</sup> Layer of PAGDs</i>	<i>The 2<sup>nd</sup> Layer of PAGDs</i>
<b>Proposed THz Absorber</b>	$T_1 = 32 \mu m$ $r_1 = 15.1 \mu m$ $H_1 = 38 \mu m$	$T_2 = 32 \mu m$ $r_2 = 8.04 \mu m$ $H_2 = 30.4 \mu m$

The spectra of the normalized input impedance of this THz absorber with the real and imaginary parts are depicted in Fig. 4, in which the imaginary part of it has been nearly adjusted zero and flat around the central frequency of 1.43 THz. Furthermore, the real part of it has been tuned approximately near 1 around this central frequency. This operation causes that the bandwidth of the absorber is increased about the central frequency.

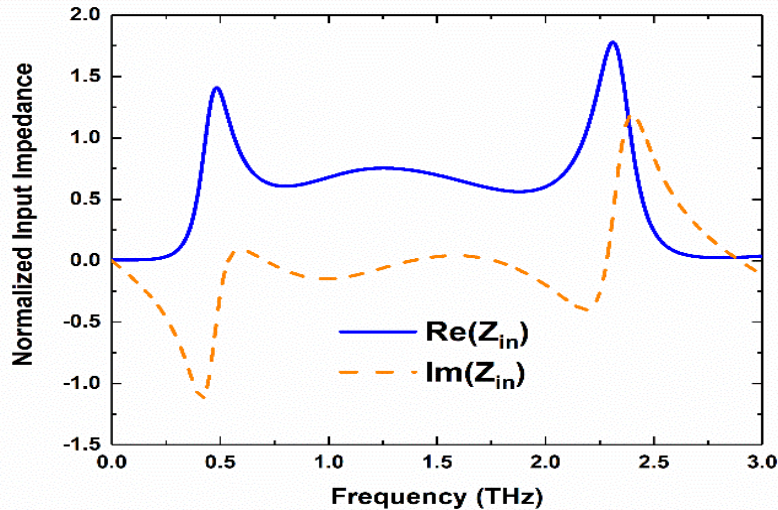


**Fig. 4.** The spectra of the real and imaginary parts of the normalized input impedance, obtained by the transmission line model and MATLAB codes.

In the next step, the accuracy of the transmission line method and the simulation is compared. The calculated spectra of the ultra-wideband absorption by the FEM (finite element method) and the deliberate transmission line model by MATLAB codes are depicted in Fig. 5. It is clear that the result of FEM and the transmission line model have an acceptable agreement in Fig. 5. As illustrated in Fig. 5(b), the obtained return loss coefficient spectra of this structure less than 0.317 are shown by the FEM and the transmission line model. As we know, the return loss

coefficient can be calculated by  $\Gamma = S_{11} = \frac{Z_{in} - Z_0}{Z_{in} + Z_0}$ . Because of the incident THz wave that cannot transmit through the golden layer, the transmission coefficient ( $S_{21}$ ) can be neglected in the absorption relationship, so it can be written as:  $A = 1 - |S_{11}|^2$ .

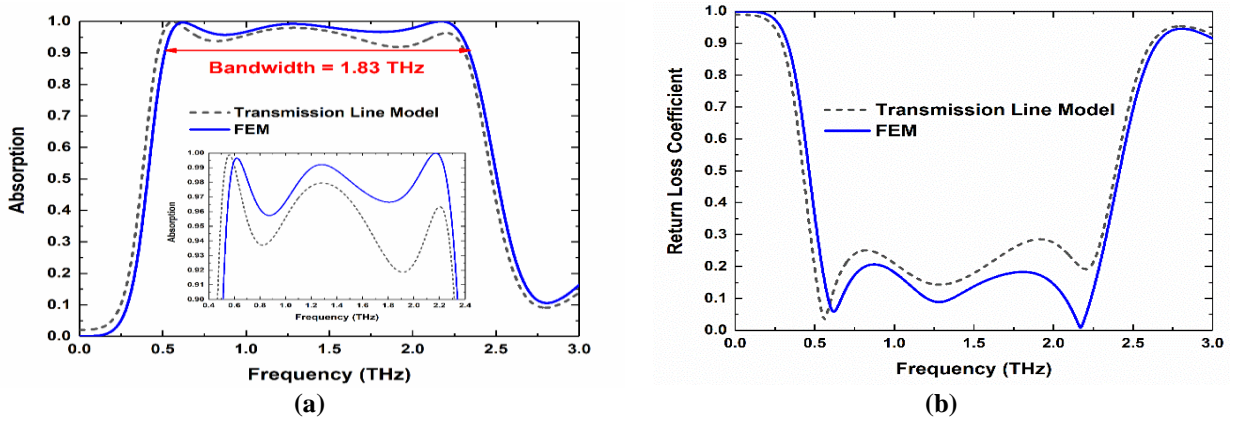


**Fig. 5. (a) The absorption spectra and their magnifying for over 90% (b) return loss coefficient of the designed device, calculated by FEM and transmission line model.**

The absorption of this device can act as functions of THz frequencies and the angle of the incident THz wave for the both Transverse Magnetic (TM) and Transverse Electric (TE) modes. In this work, we have considered the incident THz wave with the both TE and TM polarizations, and also the incident angle has been assumed with  $0^\circ$  for the both of these polarizations. In Fig. 6(a), the absorption spectra for the both TM and TE modes are demonstrated. And also, in Fig. 6(b), the return loss coefficient spectra for these modes are determined.

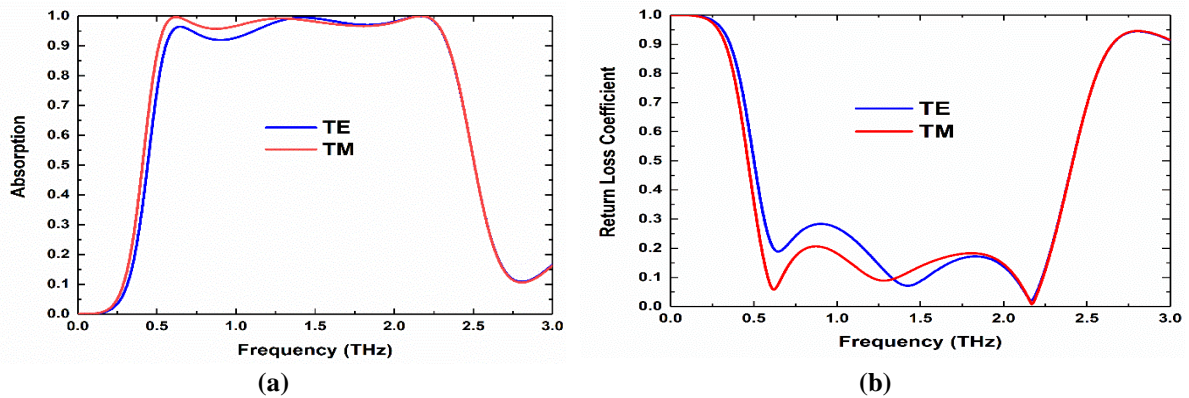


**Fig. 6. (a) Absorption (b) and return loss coefficient spectra of the proposed absorber for TM and TE polarizations of the incident THz wave, achieved by FEM.**

The vales of absorption and return loss coefficients can be controlled by Fermi levels (chemical potentials). So, in Fig. 7, the absorption and return loss coefficient spectra for various  $E_{F1}$  are depicted, and also  $E_{F2}$  has been assumed by a constant value that is equal to 0.5 eV.

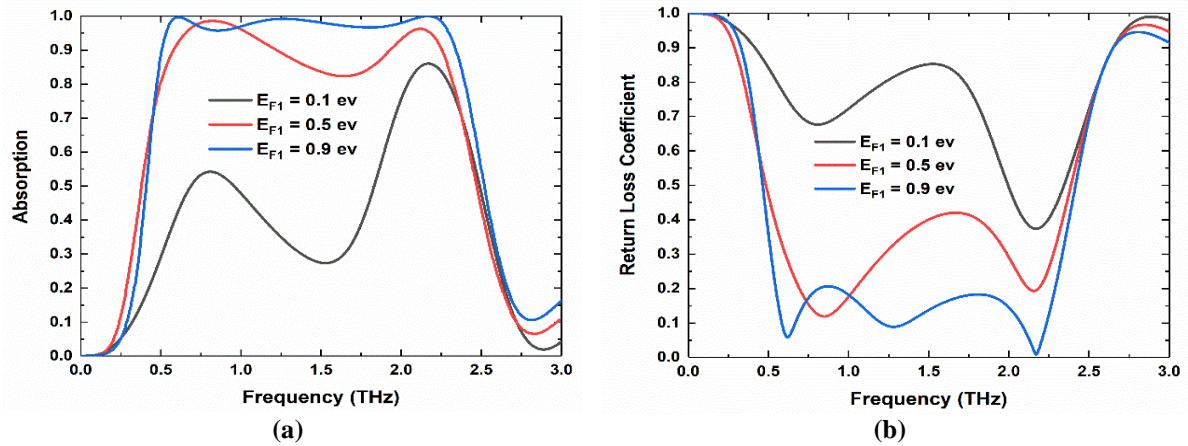


**Fig. 7. (a) Absorption (b) and return loss coefficient spectra of the proposed absorber for various  $E_{F1}$ , achieved by FEM.**

Then, in Fig. 8, the absorption and return loss coefficient spectra for various  $E_{F2}$  are shown, while  $E_{F1}$  is equal to 0.9 eV.

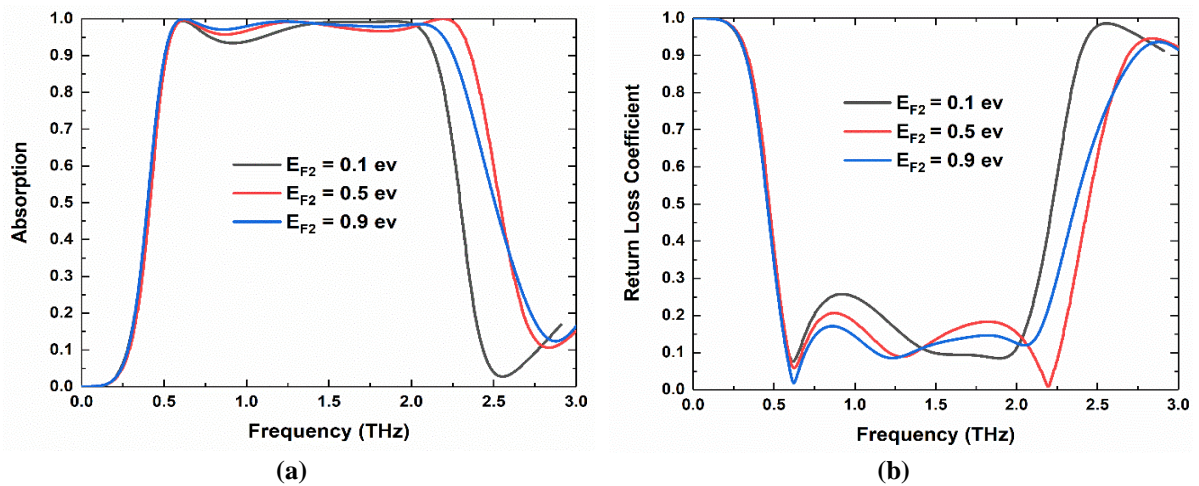


**Fig. 8. (a) Absorption (b) and return loss coefficient spectra of the proposed absorber for various  $E_{F1}$ , achieved by FEM.**

From Fig. 8(a), as a result, the best bandwidth of 90% absorption has been achieved, when  $E_{F1}$  and  $E_{F2}$  are adjusted to 0.9 eV and 0.5 eV respectively. So, the normalized bandwidth of this THz absorber is reached up to 128% with 1.43 THz of the central frequency of this absorber.

As the next step, the operation of the proposed device is analyzed in “ON” and “OFF” states, which “OFF” state is determined for  $E_{F1}$  and  $E_{F2}$  that are equal to 0 eV, and “ON” state is considered for  $E_{F1}$  and  $E_{F2}$  that are equal to 0.9 eV and 0.5 eV respectively. In Fig. 9, the absorption and return loss coefficient spectra are depicted for “ON” and “OFF” states.

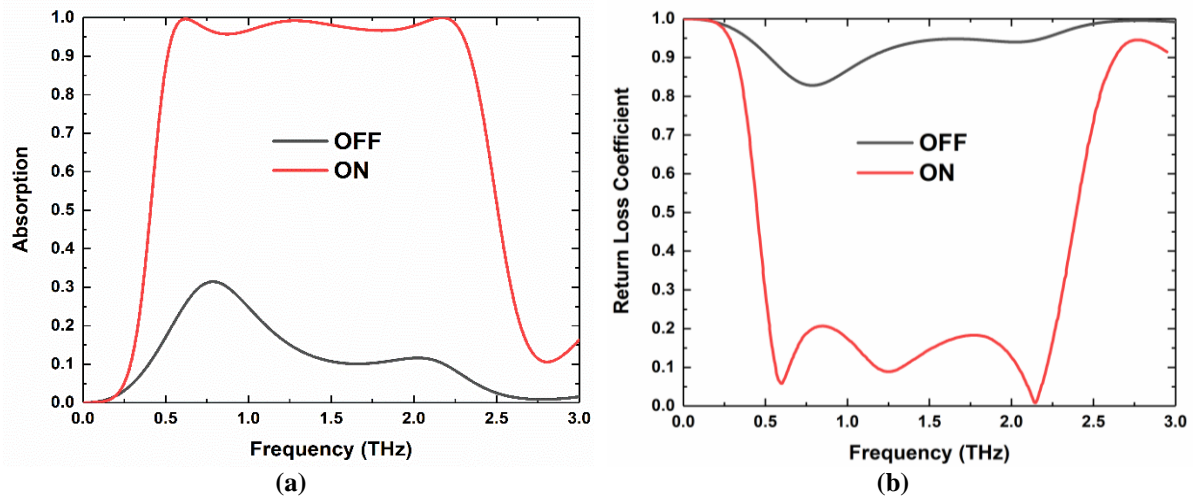


**Fig. 9.** Performance of the designed THz absorber in “ON” and “OFF” states, calculated by FEM.

As a result, the operation of our proposed ultra-wideband THz absorber and some of the best previous broadband and ultra-broadband absorbers are given in table 4, which they were published in the various papers. In this work, the normalized bandwidth ( $BW/f_0$  (%)) has been reached up to 128%, which is 28% greater than the best previous study.

**Table 4.** The Comparison of our proposed device operation with some of the previous THz absorbers.

<i>Reference</i>	<i>Number of Graphene Layers</i>	<i>Device Height(<math>\mu\text{m}</math>)</i>	<i><math>f_0</math> (THz)</i>	<i><math>BW/f_0</math> (%)</i>
[13]	5	21	1.47	78%
[12]	1	25	2	88%
[12]	1	50	1	98%
[18]	3	26.67	2.54	100%
<b><i>Our proposed device</i></b>	<b>2</b>	<b>68.4</b>	<b>1.43</b>	<b>128%</b>

## 4. Conclusion

A novel ultra-broadband absorber in the THz regime with two layers of PAGDs and two substrates that have been determined with the same materials has been proposed in this research article. The recent analytical series RLC branch that has been modeled for each layer of graphene disks was utilized. Then, the transmission line model has been developed for the whole of the absorber configuration, in which the mentioned series RLC branch was considered. And also, the transmission line model could be used for achieving the value of the input impedance of the designed absorber. Therefore, the real part of the input impedance has been adjusted to be matched about the free space impedance, on the other hand, the imaginary part of it has been approximately tuned near zero around 1.43 THz of the central frequency. And also, the thickness of graphene disks was assumed with 1 nm in this work that is approximately 10 times greater than the thickness of one graphene layer. Finally, the bandwidth of this proposed ultra-wideband THz absorber has been achieved 1.83 THz with 1.43 THz of the central frequency by FEM and transmission line model, in which the return loss coefficient has been obtained less than 10% in a THz regime.

## References

- [1] J. Wu *et al.*, "Dual-band infrared near-perfect absorption by Fabry-Perot resonances and surface phonons," *J Plasmonics* vol. 13, no. 3, pp. 803-809, 2018.
- [2] J. Yang *et al.*, "Broadband terahertz absorber based on multi-band continuous plasmon resonances in geometrically gradient dielectric-loaded graphene plasmon structure," *J Scientific reports* vol. 8, no. 1, p. 3239, 2018.
- [3] F. H. Koppens, D. E. Chang, and F. J. N. I. Garcia de Abajo, "Graphene plasmonics: a platform for strong light-matter interactions," *J Nano letters* vol. 11, no. 8, pp. 3370-3377, 2011.
- [4] F. Bonaccorso, Z. Sun, T. Hasan, and A. J. N. p. Ferrari, "Graphene photonics and optoelectronics," *J Nature photonics* vol. 4, no. 9, p. 611, 2010.

- [5] M. Chen, W. Sun, J. Cai, L. Chang, and X. J. O. C. Xiao, "Frequency-tunable terahertz absorbers based on graphene metasurface," *J Optics Communications* vol. 382, pp. 144-150, 2017.
- [6] Y. Dong, P. Liu, D. Yu, G. Li, L. J. I. A. Yang, and W. P. Letters, "A Tunable Ultrabroadband Ultrathin Terahertz Absorber Using Graphene Stacks," *J IEEE Antennas* vol. 16, pp. 1115-1118, 2017.
- [7] M. Huang, Y. Cheng, Z. Cheng, H. Chen, X. Mao, and R. J. O. C. Gong, "Based on graphene tunable dual-band terahertz metamaterial absorber with wide-angle," *J Optics Communications* vol. 415, pp. 194-201, 2018.
- [8] X.-j. He *et al.*, "Broadband and polarization-insensitive terahertz absorber based on multilayer metamaterials," *J Optics Communications* vol. 340, pp. 44-49, 2015.
- [9] S. Ke, B. Wang, H. Huang, H. Long, K. Wang, and P. J. O. e. Lu, "Plasmonic absorption enhancement in periodic cross-shaped graphene arrays," *J Optics express* vol. 23, no. 7, pp. 8888-8900, 2015.
- [10] S. Barzegar-Parizi, B. Rejaei, and A. J. I. J. o. Q. E. Khavasi, "Analytical circuit model for periodic arrays of graphene disks," *J IEEE Journal of Quantum Electronics*, vol. 51, no. 9, pp. 1-7, 2015.
- [11] M. Biabanifard, M. S. J. O.-I. J. f. L. Abrishamian, and E. Optics, "Circuit modeling of tunable terahertz graphene absorber," *J Optik-International Journal for Light and Electron Optics*, vol. 158, pp. 842-849, 2018.
- [12] A. J. J. B. Khavasi, "Design of ultra-broadband graphene absorber using circuit theory," *J JOSA B* vol. 32, no. 9, pp. 1941-1946, 2015.
- [13] J. Zhu *et al.*, "Ultra-broadband terahertz metamaterial absorber," *J Applied Physics Letters* vol. 105, no. 2, p. 021102, 2014.
- [14] A. J. J. B. Khavasi, "Design of ultra-broadband graphene absorber using circuit theory," vol. 32, no. 9, pp. 1941-1946, 2015.
- [15] L. Ye *et al.*, "Broadband absorber with periodically sinusoidally-patterned graphene layer in terahertz range," *J Optics express* vol. 25, no. 10, pp. 11223-11232, 2017.
- [16] A. Fardoost, F. G. Vanani, and R. J. I. T. o. N. Safian, "Design of a multilayer graphene-based ultrawideband terahertz absorber," *J IEEE Transactions on Nanotechnology* vol. 16, no. 1, pp. 68-74, 2017.
- [17] P. Fu, F. Liu, G. J. Ren, F. Su, D. Li, and J. Q. J. O. C. Yao, "A broadband metamaterial absorber based on multi-layer graphene in the terahertz region," *J Optics Communications* vol. 417, pp. 62-66, 2018.
- [18] B. J. O. Sadegh, "Ultra-broadband terahertz absorber based on graphene ribbons," *J Optik-International Journal for Light and Electron Optics*, vol. 172, pp. 1026-1033, 2018.
- [19] S. Biabanifard, M. Biabanifard, S. Asgari, S. Asadi, and C. J. O. C. Mustapha, "Tunable ultra-wideband terahertz absorber based on graphene disks and ribbons," *J Optics Communications* vol. 427, pp. 418-425, 2018.
- [20] M. J. A.-I. J. o. E. Şengül and Communications, "Broadband impedance matching via lossless unsymmetrical lattice networks," *J AEU-International Journal of Electronics and Communications* vol. 66, no. 1, pp. 76-79, 2012.

- [21] G. W. J. I. T. o. A. Hanson and Propagation, "Dyadic Green's functions for an anisotropic, non-local model of biased graphene," *J IEEE Transactions on Antennas Propagation*, vol. 56, no. 3, pp. 747-757, 2008.
- [22] S. J. E. Mikhailov, "Non-linear electromagnetic response of graphene," *J EPL*, vol. 79, no. 2, p. 27002, 2007.